

$^{86}\text{Kr}(d, p)^{87}\text{Kr}$ Reaction*

K. HARAVU,† C. L. HOLLAS, P. J. RILEY, AND W. R. COKER

The University of Texas at Austin, Austin, Texas 78712

(Received 11 September 1969)

States of ^{87}Kr have been investigated via the $^{86}\text{Kr}(d, p)^{87}\text{Kr}$ reaction, with 11-MeV deuterons and an over-all energy resolution of 30 keV. Proton groups leading to 23 states in ^{87}Kr have been identified. The angular-distribution data have been analyzed using finite-range distorted-wave Born-approximation (DWBA) calculations to extract spectroscopic information. Spin and parity assignments, excitation energies, and spectroscopic factors for most of the observed levels are presented. Comparisons are made with preliminary data of proton elastic scattering from ^{86}Kr at isobaric analog resonances.

I. INTRODUCTION

THE ^{86}Kr nucleus has a "magic" number of neutrons, $N=50$, and is therefore convenient for studying shell structure, in view of the expected simplicity of the final neutron configurations. Previous measurements¹⁻⁴ have been carried out on the various closed-neutron-shell ($N=50$) nuclei, ^{86}Kr , ^{88}Sr , ^{90}Zr , and ^{92}Mo . The measurements on ^{86}Kr were carried out by Sass, Schneid, and Rosner using krypton gas isotopically enriched to 95.7% ^{86}Kr , in conjunction with a magnetic spectrograph, with an over-all experimental resolution of approximately 120 keV. In the present work, krypton gas isotopically enriched to 98.5% ^{86}Kr was available, and the experimental resolution was approximately 30 keV. The higher isotopic purity and the better experimental energy resolution have allowed more accurate angular-momentum assignments and the identification of additional states in ^{87}Kr .

In addition, isobaric analogs of the low-lying states of ^{87}Kr have recently been studied by means of proton elastic and inelastic scattering measurements on ^{86}Kr at proton energies from 4.6 to 10.1 MeV.⁵ A detailed comparison of analog states in ^{87}Rb , as observed in proton-elastic-scattering measurements, with the states in ^{87}Kr observed in the (d, p) work, was therefore of interest.

II. EXPERIMENTAL PROCEDURE

$^{86}\text{Kr}(d, p)^{87}\text{Kr}$ cross sections were measured at 5° intervals at laboratory angles from 20° to 160° at an incident center-of-target deuteron energy of 10.997

MeV. The target gas, isotopically enriched to 98.5% ^{86}Kr , was contained within a 3-in.-diam gas cell⁶ used in conjunction with a 20-in.-diam scattering chamber. The cell walls were 0.00012-in.-thick Mylar. Beam entrance was through a 5/16×7/16-in. nickel foil, 10 $\mu\text{in.}$ thick; the beam exit window was a similar nickel foil 20 $\mu\text{in.}$ thick. The gas pressure was approximately 0.025 atm, corresponding to a target thickness of approximately $(80/\sin\theta_{\text{lab}})$ $\mu\text{g}/\text{cm}^2$. Two movable 2-mm-thick lithium-drifted silicon detectors, cooled to approximately dry-ice temperature, were used. The over-all experimental proton resolution was 30 keV. Proton groups leading to 23 states in ^{87}Kr were identified. Figure 1 shows typical spectra, taken at laboratory angles of 45° and 145°. The excitation energies are indicated in the figure. The $^{86}\text{Kr}(d, p)^{87}\text{Kr}$ ground-state Q value of 3.2856 ± 0.0099 MeV⁷ was used in the calculation of excitation energies. Slight contamination was present, as the spectra indicate, and it is chiefly attributed to carbon. The over-all experimental uncertainty in the measured absolute cross sections is of the order of 6% (standard deviation).

III. OPTICAL ANALYSIS

To obtain the optical parameters needed to calculate the incoming deuteron and outgoing proton distorted waves in the DWBA analysis, optical-model fits, including a spin-orbit interaction, were made to 10.997-MeV (lab) deuteron and 9.66-MeV (lab) proton elastic scattering from ^{86}Kr . The $^{86}\text{Kr}(p, p)$ data were obtained from the isobaric-analog-resonance elastic scattering work.⁵ The deuteron parameters were determined with a code written by Smith,⁸ and the proton parameters with a code written by Perey.⁹ The optical-model fits for deuteron and proton elastic scattering, and the corresponding optical parameters, are shown in Figs. 2 and 3, respectively. The fits were made using a potential with a surface-peaked imaginary part and a

* Work supported in part by the U.S. Atomic Energy Commission.

† Present address: 5 Northern Railway Colony, Sardar Patel Road, New Delhi, India.

¹ R. E. Sass, B. Rosner, and E. J. Schneid, *Phys. Rev.* **138**, 2B 399 (1965).

² E. R. Cosman, H. A. Enge, and A. Sperduto, *Phys. Rev.* **165**, 1175 (1968).

³ J. S. Forster, L. L. Green, N. W. Henderson, J. L. Hutton, G. D. Jones, J. F. Sharpey-Schafer, A. G. Craig, and G. A. Stephens, *Nucl. Phys.* **A101**, 113 (1967); B. L. Cohen and O. V. Chubinsky, *Phys. Rev.* **131**, 2184 (1963).

⁴ S. A. Hjorth and B. L. Cohen, *Phys. Rev.* **135**, B920 (1965).

⁵ C. L. Hollas, E. R. Hiddleston, V. D. Mistry, and P. J. Riley, in *Nuclear Isospin*, edited by J. D. Anderson *et al.* (Academic Press Inc., New York, 1969), p. 667.

⁶ Designed at Oak Ridge National Laboratory.

⁷ C. Maples, G. W. Goth, and J. Cerney, University of California Lawrence Radiation Laboratory Report No. UCRL-16964, 1966 (unpublished).

⁸ W. R. Smith, University of Southern California Report No. 136-119, 1967 (unpublished).

⁹ F. G. Perey (private communication).

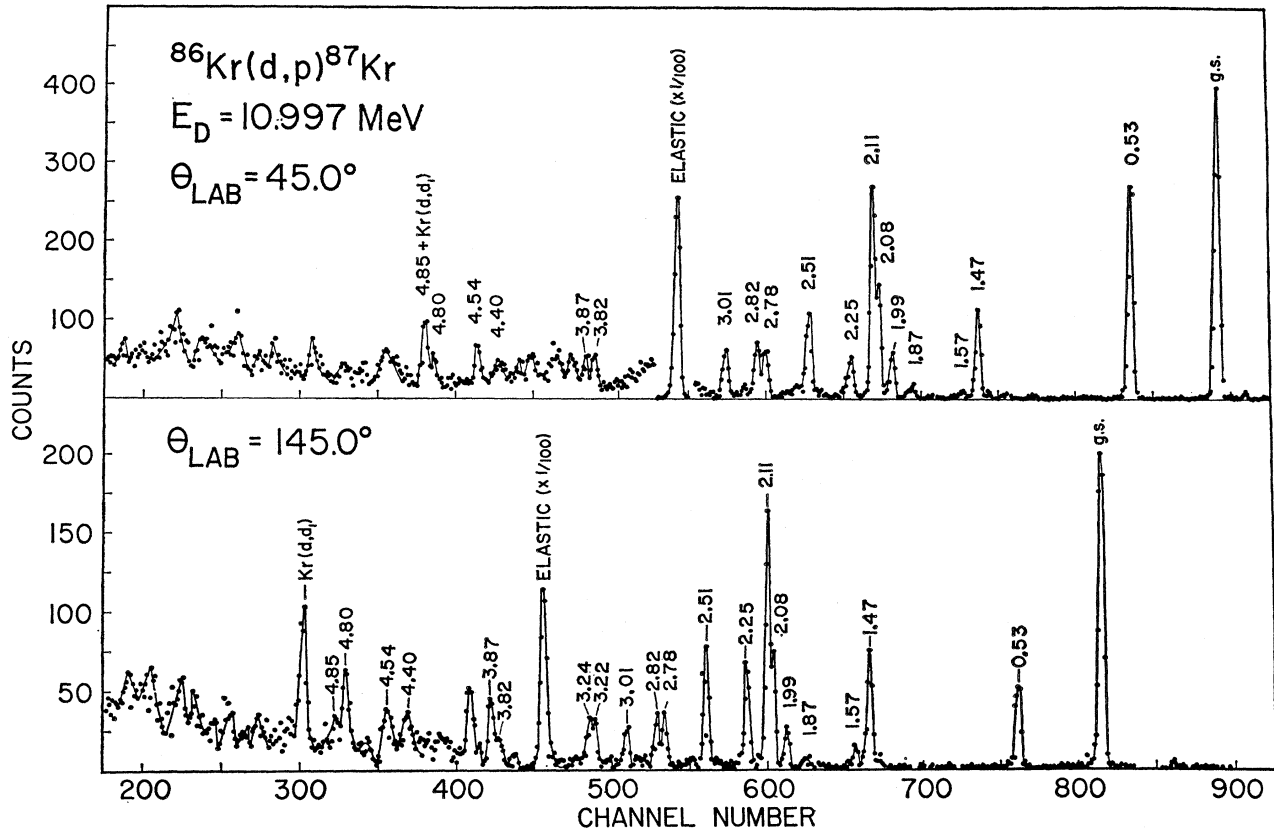


FIG. 1. $^{86}\text{Kr}(d,p)^{87}\text{Kr}$ pulse-height spectra, at a deuteron energy of 10.997 MeV and laboratory angles of 45° and 145° .

real Thomas-type spin-orbit part:

$$\begin{aligned}
 V(r) = & -Vf(r, r_0, a_r) + iAa_i W_D(d/dr)f(r, r_0, a_i) && \text{Central} \\
 & + \sigma \cdot \mathbf{I} V_{so} (\hbar/m_\pi c)^2 r^{-1} (d/dr)f(r, r_0, a_r) && \text{Spin-orbit} \\
 & + (Ze^2/2rc)(3-r^2/rc^2), && \text{if } r \leq rc \\
 & + Ze^2/r, && \text{if } r > rc. && \text{Coulomb}
 \end{aligned}$$

The function $f(r, r_0, a)$ is the usual Saxon-Woods shape:

$$f(r, r_0, a) = [1 + \exp(r - r_0 A^{1/3})/a]^{-1}.$$

The deuteron optical analysis was made by starting with the parameters obtained from deuteron elastic scattering from ^{88}Sr ,² and searching on them. The proton analysis was made beginning with Perey's average parameters.¹⁰ Since the protons emitted in the various (d, p) reactions all have an energy different from that at which this fit was made, an energy extrapolation of the real proton well depth was actually used in the DWBA analysis.

The extrapolation procedure was as follows: Holding all other parameters fixed, the real well depth V for the proton was varied away from the value of 57.09 MeV

obtained for an incident proton energy of 9.76 MeV, until the fit to the $^{86}\text{Kr}(d, p)^{87}\text{Kr}$ ($d_{5/2}$ ground state) angular distribution was optimized. The resulting energy dependence is $V = (69.36 - 1.26E_p)$ MeV. A slight energy dependence was also obtained for the proton-surface imaginary well depth W_D by repeating the procedure of optimizing the ground-state (d, p) fit. The expression $W_D = (10.57 + 0.20E_p)$ MeV was used.

IV. DWBA ANALYSIS

The (d, p) data were fitted using a zero-range DWBA program VENUS written by Tamura,¹¹ and modified to include an approximate finite-range correction.¹² The finite-range correction was found to have a negligible effect on the spectroscopic factors for all

¹¹ T. Tamura, Comp. Phys. Commun. (to be published).

¹² P. A. Moore, P. J. Riley, C. M. Jones, M. D. Mancusi, and J. L. Foster, Phys. Rev. **175**, 1516 (1968).

¹⁰ F. G. Perey, Phys. Rev. **131**, 745 (1963).

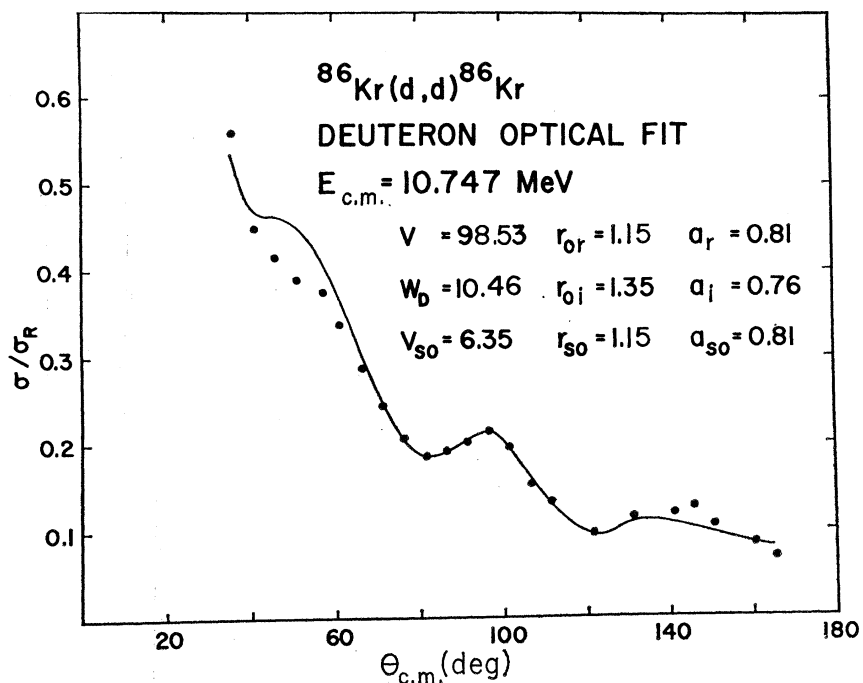


FIG. 2. Optical-model fit to $^{86}\text{Kr}(d,d)$ elastic scattering data. The cross section is shown as a ratio to the corresponding Rutherford cross section.

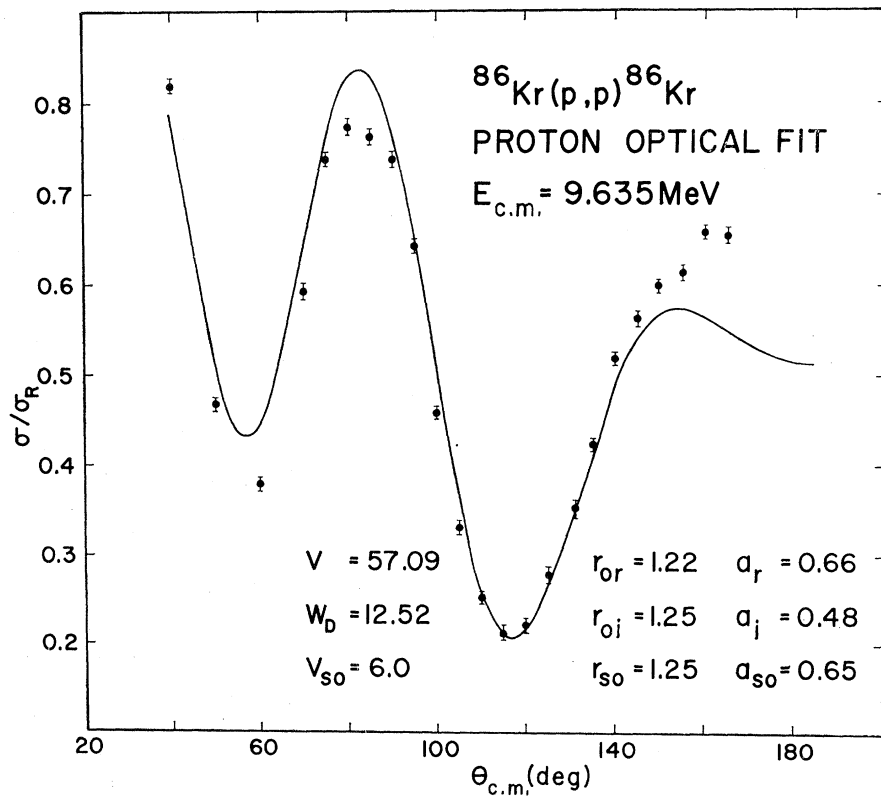


FIG. 3. Optical-model fit to $^{86}\text{Kr}(p,p)$ elastic scattering data. The cross section is shown as a ratio to the corresponding Rutherford cross section.

TABLE I. Levels of ^{87}Kr from the $^{86}\text{Kr}(d, p)^{87}\text{Kr}$ reaction. E^* is the excitation energy of the observed levels in ^{87}Kr ; l_n is the orbital angular momentum of the transferred neutron; J and π are the assumed spin and parity of the observed levels in ^{87}Kr , as suggested by the expected shell-model ordering; $d\sigma/d\Omega$ is the laboratory differential cross section; and S_J is the calculated spectroscopic factor as defined in the text. The columns at the extreme right indicate corresponding isobaric analog resonances observed in the $^{86}\text{Kr}+p$ reaction. E_R (c.m.) - 5.35 MeV gives the excitation of the analog resonance, and l_p is the transferred orbital angular momentum.

$^{86}\text{Kr}(d, p)^a$					$^{86}\text{Kr}(d, p)^b$					$^{86}\text{Kr}(p, p)^c$	
E^* (MeV)	l_n	J^π	$d\sigma/d\Omega$ (max) (mb/sr)	S_J	E^* (MeV)	l_n	J^π	$d\sigma/d\Omega$ (max) (mb/sr)	S_J	E_R (c.m.) - 5.35 MeV	l_p
0.00	2	$\frac{5}{2}^+$	9.35	0.56	0.00	2	$\frac{5}{2}^+$	15.2	0.66	0.00	2
0.529	0	$\frac{1}{2}^+$	6.41 ⁺	0.46	0.55	0	$\frac{1}{2}^+$	4.7	0.67	0.53	0
1.468	2	$\frac{3}{2}^+$	2.98	0.23	1.52	2	$\frac{3}{2}^+$	5.7	0.31	1.47	2
1.468	2	$\frac{5}{2}^+$	2.98	0.14							
1.570			0.14								
1.873	(2)	($\frac{3}{2}$)	0.21	0.02						1.88	(2)
1.996	2	$\frac{3}{2}^+$	1.78	0.09						2.00	2
2.080	0	$\frac{1}{2}^+$		0.18						2.07	0
			8.92								
2.112	2	$\frac{3}{2}^+$		0.30	2.17	2	$\frac{3}{2}^+$	10.9	0.53	2.11	2
2.250	(5)	($\frac{1}{2}^-$)		0.18						2.27	5
			1.23								
2.277	(0)	($\frac{1}{2}^+$)		0.03							
2.515	4	$\frac{7}{2}^+$	1.24	0.49	2.57	(2+4)	$\frac{3}{2}^+, \frac{7}{2}^+$	3.5		2.54	4
2.775	2	$\frac{3}{2}^+$	1.34	0.10						2.79	2
2.775	2	$\frac{5}{2}^+$	1.34	0.05							
2.823	2	$\frac{3}{2}^+$	1.15	0.11	2.89	2	$\frac{3}{2}^+$	5.5	0.26		
										2.91	(2)
3.015	2	$\frac{3}{2}^+$	0.92	0.08	3.09	2	$\frac{3}{2}^+$	3.4	0.14		
3.223	2	$\frac{3}{2}^+ + \frac{3}{2}^+$		0.12							
			0.67		3.31	(0+2)	$\frac{1}{2}^+, \frac{3}{2}^+$	2.2			
3.237	2	$\frac{5}{2}^+ + \frac{5}{2}^+$		0.08							
3.552					3.65	2	$\frac{3}{2}^+$	2.4	0.10		
3.819											
3.871					3.97						
4.402											
4.536											
4.800											
4.856											
+35° point											

^a Present work.

^b Reference 1.

^c Reference 5.

residual states. The bound-state neutron wave functions needed for the analysis were calculated from code NEPTUNE, also by Tamura.¹¹ The Woods-Saxon well for the bound state was assumed to have the standard geometry, $r_0=1.25$ fm, and $a=0.65$ fm. The spin-orbit depth was taken to be 6.0 MeV, and the spin-orbit geometry was taken to be the same as the central potential geometry. The binding energy of each level was held fixed at the experimentally determined separation energy, and a search was made for the Woods-Saxon well depth which bound such a state at that energy.

The $d_{5/2}$, $d_{3/2}$, and $s_{1/2}$ levels were bound by a depth of around 49.0-50.0 MeV, except for the highly excited $d_{3/2}$ states for which the depth had to be decreased to

47.0 MeV. The $g_{7/2}$ was bound using 47.0 MeV, and the $h_{11/2}$ required 54.1 MeV.

The experimental angular distributions, and their comparison with DWBA predictions, are shown in Figs. 4(a), 4(b), and 4(c). Where error bars are not used, the size of the data point indicates the approximate statistical error in the cross sections. There is over-all agreement between experiment and theory. Since ^{86}Kr is an even-even nucleus, the general relationship between the experimental absolute $^{86}\text{Kr}(d, p)^{87}\text{Kr}$ cross section and the theoretical cross section for forming a state with spin J is given by

$$\sigma(\text{expt}) = (2J+1)\sigma_{\text{DWBA}}S_J.$$

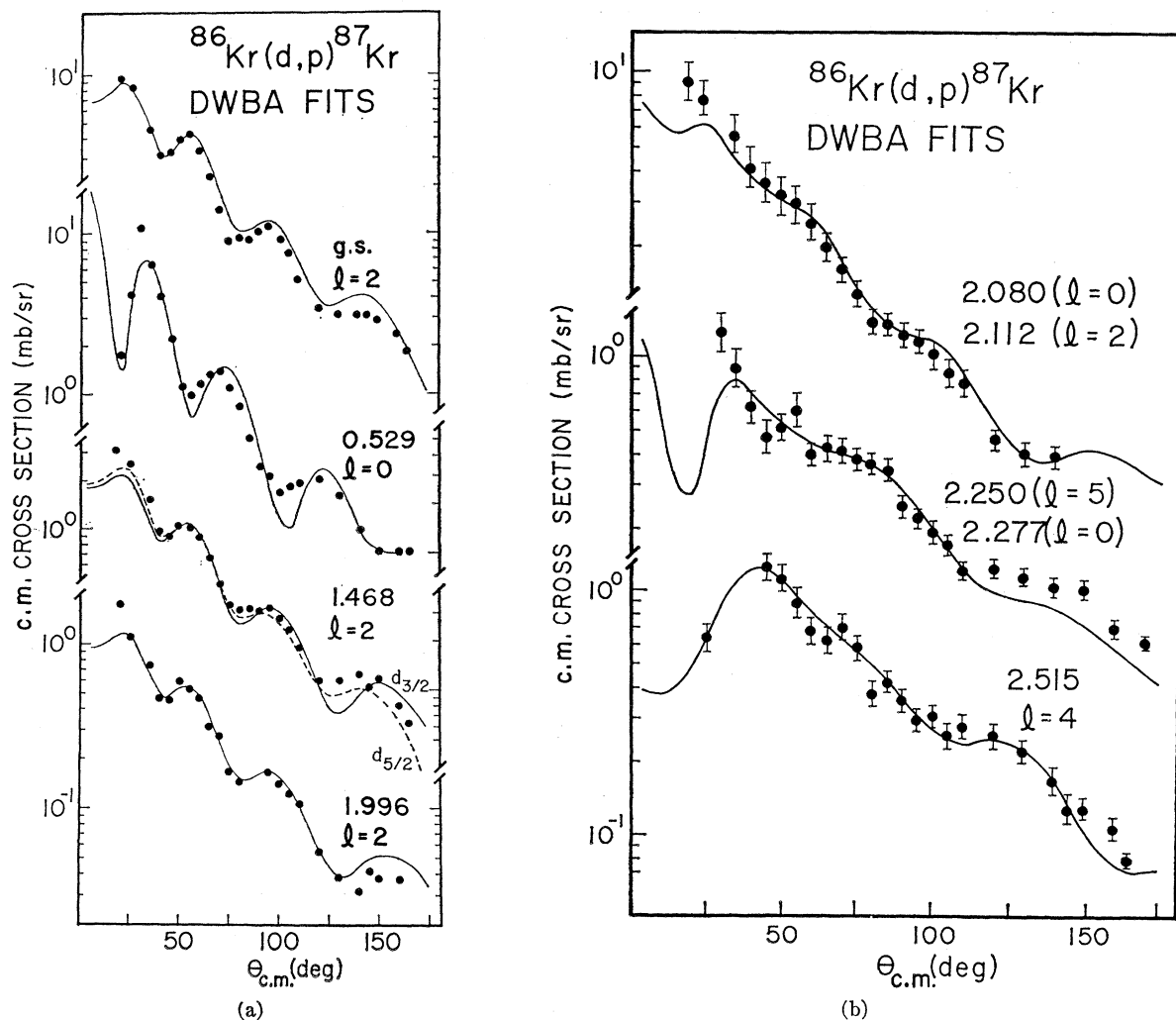


FIG. 4. DWBA fits to $^{86}\text{Kr}(d, p)^{87}\text{Kr}$ angular-distribution data. The l_n values and excitation energies are as indicated. Where error bars are not used, the size of the data point indicates the approximate statistical error in the cross sections.

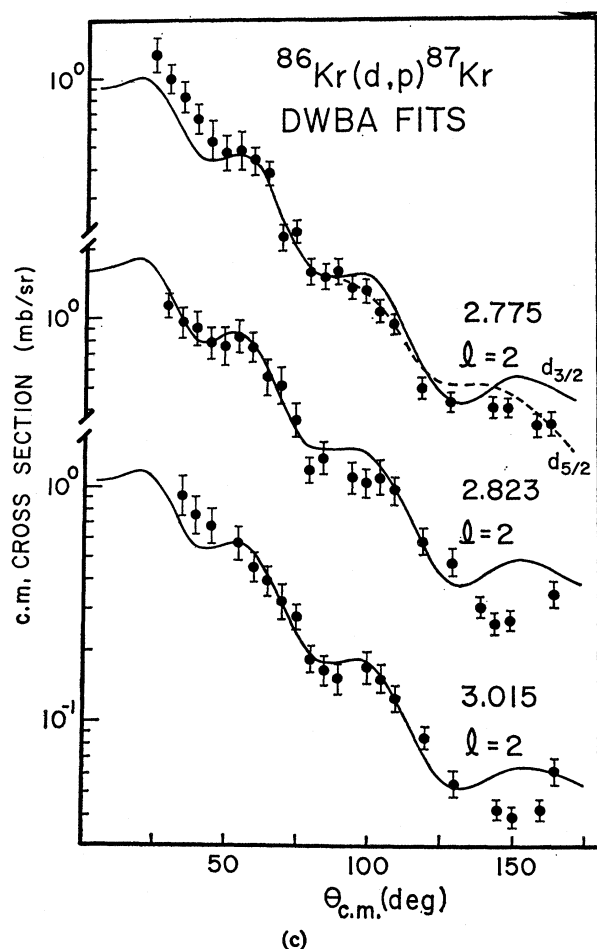
We have taken the absolute theoretical cross section σ_J (theory) to be $(2J+1)\sigma_{\text{DWBA}}$, so that the spectroscopic factor S_J is defined by the ratio

$$S_J = \sigma(\text{expt}) / \sigma_J(\text{theory}).$$

Values of the spectroscopic factor were obtained by normalizing the theoretical cross sections at forward angles to the experimental data.

Table I shows the present work compared both with that of Sass, Rosner, and Schneid,¹ and also with preliminary $^{86}\text{Kr}(p, p)$ measurements taken over isobaric analog resonances.⁵ Many states were unresolved in the earlier (d, p) work; thus, a detailed comparison for states above the second excited state of ^{87}Kr is difficult. In the present work, the states at 2.080 ($l=0$) and 2.112 ($l=2$) MeV constitute an unresolved doublet, as do those at 2.250 ($l=5$) and 2.277 ($l=0$) MeV. The weak $l=0$ state at 2.277-MeV excitation is partially resolved from the 2.250-MeV state only at the more

forward angles in the spectra. The weak state at 1.57 MeV could not be analyzed; a study of the incomplete angular distribution for the 1.87-MeV state gives $l=2$. It was not possible to obtain complete angular distributions for the states at excitations of 3.223, 3.237, and 3.552 MeV because of the presence of the deuteron elastic peak in the spectra. In addition, because of the rather large uncertainty in the cross sections of the more highly excited states, DWBA fits were not attempted for states of excitation higher than 3.24 MeV. The spectroscopic factor for the ground state is 0.56, 16% lower than the value of 0.66 obtained by Sass, Rosner, and Schneid.¹ The spectroscopic factors for the first and second excited states are also very similar to those obtained in the earlier work. The 37% discrepancy in the spectroscopic factor $S_J=0.46$ for the first excited state at 0.529 MeV, observed in the present work, as compared with the value $S_J=0.67$ obtained by Sass *et al.*, is probably due to the fact that the most



(c)
FIG. 4. (Continued).

forward angle in the present work was 20° , so that the second maximum in the angular distribution was used for normalization. In the previous work, the data extended forward to approximately 12° , allowing a more meaningful comparison between theory and experiment. Only resonance energies and l -value assignments are available in the elastic scattering work; however, it is clear that, in general, there is excellent agreement between the present (d, p) and the (p, p) work.

Spin assignments to the states of ^{87}Kr were made on the basis of the conventional shell-model ordering of states, and on the results of polarization measurements of proton elastic scattering from ^{88}Sr at analog resonances.^{13,14} The spin of the ground state of ^{89}Sr was found to be $\frac{5}{2}^+$, and those of the successive low-lying states were found to be $\frac{1}{2}^+$, $\frac{3}{2}^+$, $\frac{3}{2}^+$, $\frac{3}{2}^+$, $\frac{7}{2}^+$, respectively. The very weak second excited state of ^{89}Sr , for which the assignment $d_{5/2}$ has tentatively been given, is believed to be built from the coupling of $(d_{5/2})_n$ to the first

¹³ J. L. Ellis and W. Haerberli, in *Nuclear Isospin*, edited by J. D. Anderson *et al.* (Academic Press Inc., New York, 1969), p. 585.

¹⁴ G. Clausnitzer, R. Fleischmann, G. Graw, and K. Wienhard, in *Nuclear Isospin* edited by J. D. Anderson *et al.* (Academic Press Inc., New York, 1969), p. 629.

excited state of ^{88}Sr , and it is not clear whether a similar state is observed in ^{87}Kr in the present work. It seems reasonable to assign to all the $l=2$ states observed in the present work, except for the ground state, the spin and parity $\frac{3}{2}^+$. However, the assignment $d_{5/2}$ gives a markedly better fit to the data than does $d_{3/2}$ for both the 1.468- and 2.775-MeV $l=2$ states, as can be seen in Fig. 4. The dashed line is the $d_{5/2}$ fit, the solid line the $d_{3/2}$ fit. The difference in the quality of the fits is most noticeable past 100° .

The spectroscopic factors extracted for the doublets at 2.080, 2.112, 2.250, and 2.277 MeV, should be considered to have a higher uncertainty than the other figures given in Table I. Since the doublets were often not resolved, they were summed together and spectroscopic factors were extracted by solving

$$\sigma(\text{expt}) = S_1\sigma_1(\text{DWBA}) + S_2\sigma_2(\text{DWBA})$$

at several pairs of angles. A cursory analysis was given the doublet at 3.223, 3.237 MeV, with both states assumed to have the same angular momentum ($l_n=2$); however, the experimental angular distribution for this doublet is too incomplete for meaningful analysis, and the net spectroscopic factor is given in Table I merely for purposes of indicating the approximate strength of the transition.

V. CONCLUSIONS

Of the 16 states in ^{87}Kr observed via (d, p) at excitations of less than 3.25 MeV, three (at 0.53, 2.08, and 2.28 MeV) are assigned $l_n=0$, nine are assigned $l_n=2$, and solitary $l_n=4$ and $l_n=5$ levels are observed. The two remaining states (at 1.570 and 1.873 MeV) had cross sections too small to permit reliable analysis.

The sum of spectroscopic factors for the $s_{1/2}$ states is seen from Table I to be 0.67. It becomes 0.88 if the spectroscopic factor obtained by Sass *et al.*¹ for the 0.53-MeV state is used rather than our value. For the $d_{5/2}$ states, the sum is 0.56–0.75, depending on whether the 1.47- and 2.77-MeV states are assigned $d_{5/2}$ or not. For the $d_{3/2}$ states, the sum is 0.70–1.03, depending again on the assignments of the 1.47- and 2.77-MeV states.

Figure 5 shows a comparison of the low-lying states observed in ^{87}Kr , ^{89}Sr , ^{91}Zr , and ^{93}Mo . The lengths of the horizontal lines, representing states, correspond roughly to the relative differential cross sections observed at forward angles in (d, p) . The numeral at the right of each level is the assigned l_n value. Reading from left to right, the proton number increases by two each time, from 36 to 42, and the effect of this increase is apparent on the level spacing and ordering.

Twenty-three states in ^{87}Kr were observed in this work, and spectroscopic information has been extracted for 13 of them. A detailed comparison with ^{86}Kr proton elastic scattering over isobaric analog resonances is presently being carried out, and the results will be given elsewhere. A preliminary comparison between the (d, p) and proton-elastic-scattering measurement

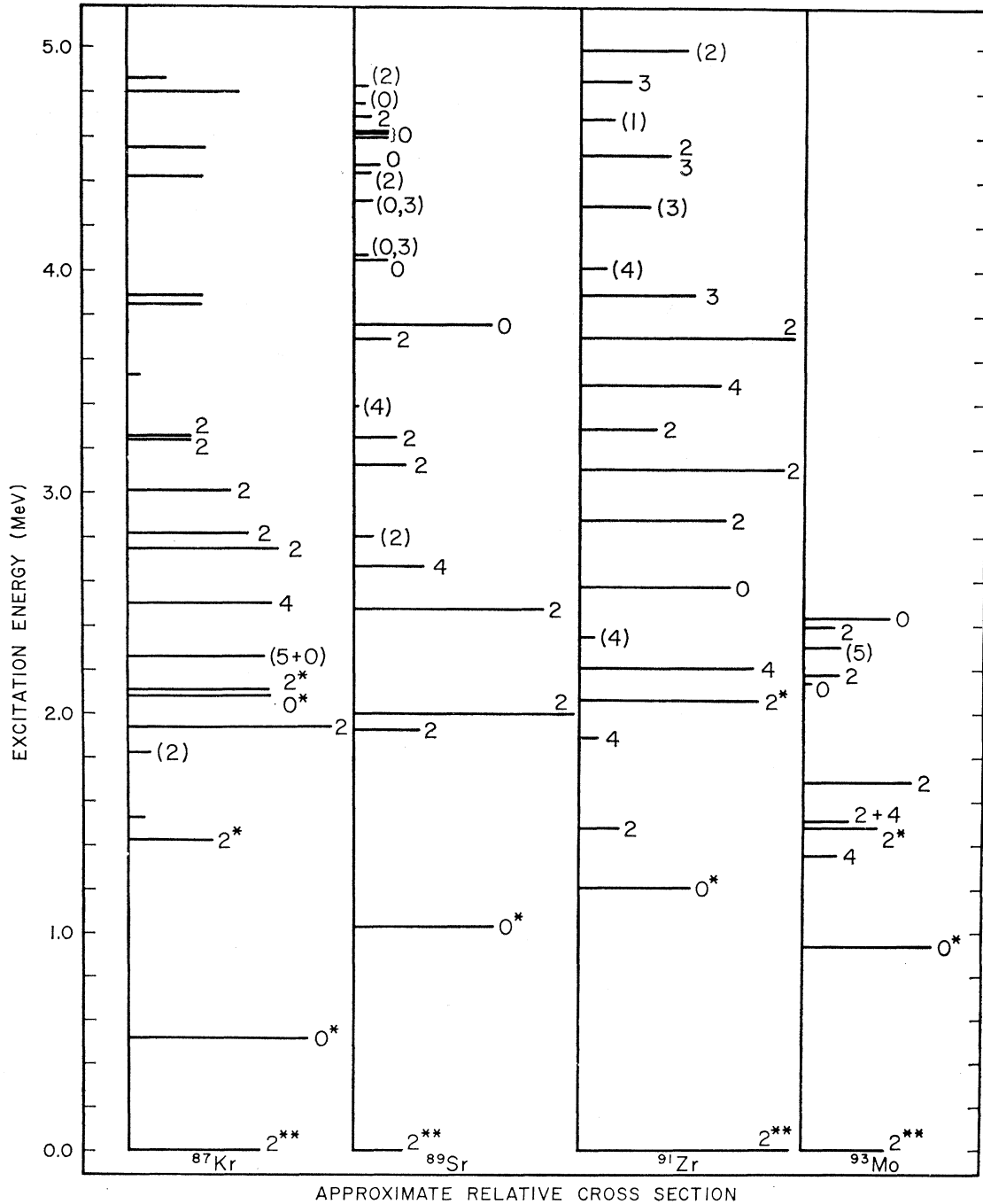


FIG. 5. A comparison of low-lying levels of ^{87}Kr , ^{89}Sr (Ref. 2), ^{91}Zr (Ref. 3), and ^{93}Mo (Ref. 4). The lengths of the horizontal lines, representing states, correspond roughly to the relative differential cross sections observed at forward angles in (d, p) measurements. l_n values are indicated by numerals. $**$ indicates $\frac{1}{6} \times (d\sigma/d\Omega)$, and $*$ indicates $\frac{1}{4} \times (d\sigma/d\Omega)$.

indicates excellent agreement. The questions raised in this study concerning the proper j assignment of various $l_n=2$ levels can be resolved using proton-elastic-polarization measurements on the isobaric analog resonances, for example.

ACKNOWLEDGMENTS

The authors wish to thank Dr. V. D. Mistry and H. R. Hiddleston for helpful discussions and for assistance in the reduction of the data.